Quantum Electronics **38** (11) 1009 – 1015 (2008)

PACS numbers: 42.55.Lt; 42.60.Lh
DOI: 10.1070/QE2008v038n11ABEH013808

Pulse repetition rate in a self-contained strontium ion laser

A.N. Soldatov, N.A. Yudin, A.V. Vasil'eva, Yu.P. Polunin,
G.D. Chebotarev, E.L. Latush, A.A. Fesenko

***Abstract*. The frequency and energy parameters of self-contained strontium ion laser ($\lambda = 1.033$ and 1.091 μm) are studied upon excitation by an additional pulse before each excitation pulse. The kinetics of processes in the active medium of this laser is numerically simulated. It is shown that the pulse repetition rate of the self-contained strontium laser can achieve $\sim$ 1 MHz. It is found that the laser pulse energy in the first pulse and the average output power and efficiency increase in a certain range of time delays between the additional and excitation pulses, which is caused by the significant prepulse concentration of strontium ions which had no time to recombine. The outlook for the application of pulse trains to excite self-contained IR transitions in strontium ions is shown.**

Keywords: *self-contained strontium laser, repetitively pulsed regime, mathematical simulation.*

A self-contained strontium ion laser emitting at 6.456 and $\sim$ 3 μm (Sr I) and $\sim$ 1 μm (Sr II) is an efficient IR radiation source [1 – 5]. The emission wavelengths of the strontium-vapour laser (SVL) fall into the absorption bands of polymers and biological tissues. The large absorption coefficient of laser radiation at these wavelengths provides efficient ablation, which allows the application of this laser in medical devices and for material processing [6].

The high energy parameters (total output power of 13.5 W and the pulse energy of 1.16 mJ [5]) and high pulse repetition rates (up to 100 kHz [7]) of SVLs stimulate further studies of these lasers with the aim of increasing their energy parameters at transitions in Sr I and Sr II at high pulse repetition rates. Strontium-vapour lasers belong to the class of RM lasers (resonance – metastable level-transition lasers). One of the most efficient RM lasers is a copper-vapour laser (CVL), which has been studied in many papers (see, for example, [8 – 12]). Among the factors limiting the achievable pulse repetition rate in CVLs (by neglecting the overheating of the active medium) are the high prepulse population of metastable states reducing the inversion and amplification [13 – 17] and prepulse electron concentration n_e, not allowing the rapid heating of the electronic gas up to temperature T_e at which the rate of population of the upper laser level exceeds that of the lower one [18 – 26]. In this case, different factors are interrelated [16] and their contributions depend on the conditions and method of exciting the active medium [25]. The ambiguity in the estimates of achievable frequency and energy characteristics even for the most thoroughly studied CVL reported in the literature necessitates further studies of RM lasers with the aim of elucidating the energy potential of these lasers and, in particular, of lasers on self-contained transitions in strontium atoms and ions.

In this paper, we studied frequency and energy characteristics of a self-contained strontium laser ($\lambda = 1.033$ and 1.091 μm) excited by an additional pulse before each excitation pulse and performed the numerical simulation of the kinetics of processes proceeding in the active medium under experimental conditions used in the study.

Experiments were performed with a self-heating gas-discharge tube (GDT) with a discharge channel made of a 50-cm-long BeO ceramic tube with the internal diameter 1.5 cm. The electrodes were mounted at the ends of the discharge channel in cold buffer zones of the GDT. Helium at a pressure of 100 Torr was used as a buffer gas. The repetitively pulsed regime of two-pulse excitation of the active medium was achieved by using a discharge of storage capacitors by thyratrons: the excitation pulse – by a TGI1-500/20 thyratron and the additional pulse – by a TGI1-270/12 thyratron. The energy of the excitation and additional pulses was changed by varying the voltage across high-voltage rectifiers, the initial voltage across storage capacitors being twice as large as that across rectifiers due to the use of the resonance charge scheme in each channel. The excitation pulse repetition rate was varied from 15 to 19 kHz. The current and laser pulses were recorded with a current shunt and a FEK-24 coaxial photocell, respectively. The detected signals were fed to a Tektronix TDS-3032 oscilloscope. The average output power was controlled with an Ophir Nova-II power meter. Emission spectra were studied by using light filters transmitting radiation at $\sim$ 1 μm (SZS-20) and at $\sim$ 3 μm (SZS-8).

A.N. Soldatov West-Siberian Branch, Russian State University of Innovation Technologies and Enterprise, prosp. Lenina 36, 630050 Tomsk, Russia; Tomsk State University, prosp. Lenina 36, 630050 Tomsk, Russia; e-mail: general@tic.tsu.ru;
N.A. Yudin West-Siberian Branch, Russian State University of Innovation Technologies and Enterprise, prosp. Lenina 36, 630050 Tomsk, Russia;
A.V. Vasil'eva, Yu.P. Polunin Tomsk State University, prosp. Lenina 36, 630050 Tomsk, Russia;
G.D. Chebotarev, E.L. Latush, A.A. Fesenko Department of Physics, Southern Federal University, ul. Zorge 5, 344090 Rostov-on-Don, Russia; e-mail: latush@phys.ru

Received 30 January 2008
Kvantovaya Elektronika **38** (11) 1009 – 1015 (2008)
Translated by I.A. Ulitkin

At the first stage of the experiment, the SVL was pumped by the excitation pulse to produce simultaneous emission at 6.456, 2.60, 2.92, 3.01 and 3.06 μm (Sr I) and at 1.033 and 1.091 μm (Sr II) with a total output power of ~ 1 W. Then, an additional pulse was applied to the GDT before each excitation pulse with a controllable delay of $\sim 1-3$ μs [27]. The output voltage of a high-voltage rectifier could be varied from 0 to 3.6 kV and the capacitance of a storage capacitor in the additional channel could be 500, 890, and 1650 pF. The voltage of a high-voltage rectifier (3.6 kV), the capacitance of a storage capacitor (890 pF) in the excitation pulse formation channel, and the capacitance of a peaking capacitor (90 pF) were not changed.

Our study showed that when the delay between the additional and excitation pulses was decreased (for comparable energies of both pump pulses), the output energy at self-contained transitions in Sr I atoms and SR II ions in the additional pulse did not change. In this case, we observed a rapid decrease in the output energy at self-contained Sr I transitions in the excitation pulse*. At the same time, in a certain range of time delays the output energy at self-contained Sr II transitions in the excitation pulse increased. This is illustrated by Fig. 1 which shows the oscillograms of discharge current pulses and laser pulses at self-contained IR transitions in Sr II [$\lambda = 1.033$ and 1.091 μm (see the energy level diagram of SR II in Fig. 2)] in the presence of only the excitation pulse and during the two-pulse excitation with the delay between the additional and excitation pulses 2.6 and 1.35 μs (capacitances of storage capacitors in the additional and main excitation channels were the same and equal to 890 pF, voltages across the rectifiers were 3.4 and 3.6 kV, respectively).

Along with the increase in the energy characteristics in the excitation pulse upon two-pulse excitation (Fig. 1), we also observed an increase in the average output power $P_{\text{av}} = 82$ at the IR transitions in Sr II. Thus, if only the 82-mW excitation pulse was used, the average output power increased to 211 mW (for a 2.6-μs delay) and to 100 mW (for a 1.35 μs delay) during the two-pulse excitation. This indicates the increase in the lasing efficiency upon two-pulse excitation and the average efficiency for both pulses.

Note that the possibility to increase the pulse energy characteristics in the second and next pulses as well as the efficiency and the average output power at recombination laser Sr II transitions in the visible range [$\lambda = 430.5$ and 416.2 nm (see Fig. 2)] upon excitation of the active medium by pulse trains with a short interpulse interval (~ 1 μs) was demonstrated in [28]. Information on the emission mechanisms of a recombination $He-Sr^{+}$ laser can be found in papers [11, 12, 29, 30]. Based on the results obtained in this paper, we can conclude that the use of pulse trains to excite self-contained IR transitions in Sr II ($\lambda = 1.033$ and 1.091 μm) is promising. In this case, to prevent the overheating of the active medium as the number of pulses in the train increases, it is necessary to decrease within the certain limits either the pulse energy input or the repetition rate of pulse trains. Preliminary experiments performed in the excitation regime by trains of three pulses with a short interpulse interval ($\sim 1-3$ μs) showed that, as in the case of recombination laser Sr II transitions [28], the pulse energy characteristics of lasing at self-contained IR transitions in Sr II in the second and third pulses exceed their values in the first pulse in a certain range of interpulse intervals.

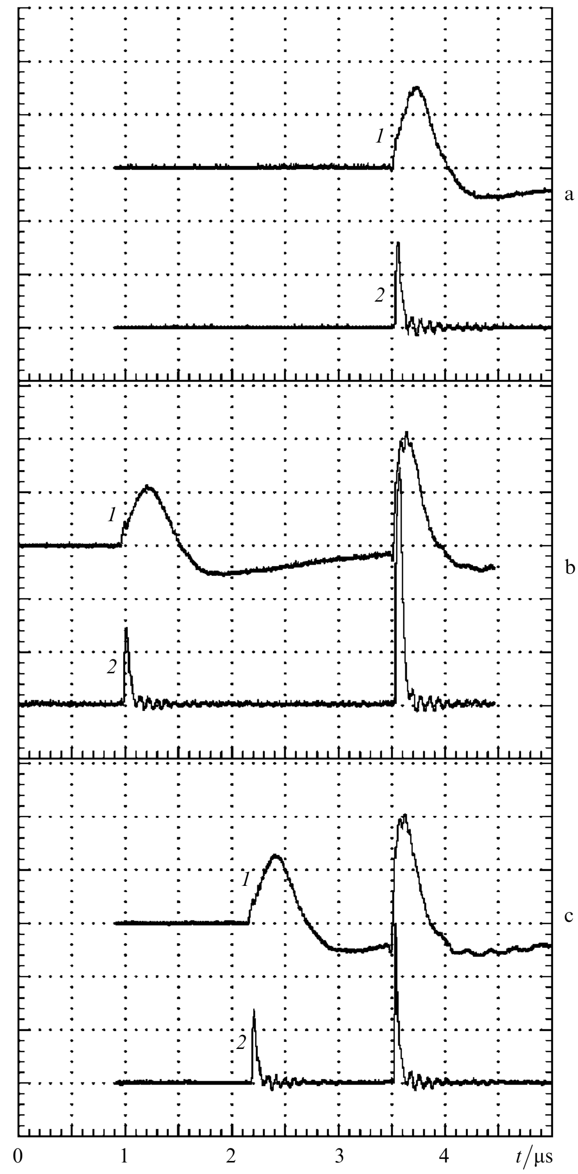

Figure 1. Oscillorams of discharge current pulses (*1*) and laser pulses at self-contained IR transitions in Sr II ($\lambda = 1.033$ and 1.091 μm) (*2*) upon single-pulse excitation (a) and two-pulse excitation with delays of 2.6 (b) and 1.35 μs (c) between the additional and excitation pulses. The scale factor for current pulses is 133 A div^{-1}.

To interpret the obtained experimental results, we simulated the kinetics of processes proceeding in the active medium. The calculations were performed by using a self-consistent mathematic model of a $He-Sr^{+}$ laser [31]. The model includes the combined description of the electric circuit and repetitively pulsed discharge plasma. The simulation of the electric circuit is reduced to the derivation of differential equations for currents and voltages, which are solved together with the kinetic equations for the plasma parameters. The kinetics of long-lived plasma components in the model is calculated taking into account the following

*It is obvious that we are dealing here not with the excitation pulse and the additional pulse (pump pulses) but with the laser radiation pulses (or 'amplification' pulses) appearing under the action of corresponding pump pulses. However, below we will speak for simplicity about laser pulses and 'amplification' pulses in the excitation, additional and other pulses.

plasmo-chemical processes: elastic and inelastic electron–atom and electron–ion collisions, collisions of metastable helium atoms leading to their ionisation, the charge exchange of atomic and molecular helium ions on strontium atoms accompanied by the production of doubly charged strontium ions, the Penning ionisation of strontium atoms by metastable helium atoms, the triple recombination of ions, the dissociative recombination of molecular ions, the conversion of atomic ions into molecular ones, the step Penning process and step charge exchange, and the diffusion of charged and metastable particles.

We calculated the level kinetics of strontium ions by taking into account 20 excited levels, shown in Fig. 2 (this figure also presents the numbers of the Sr II levels used in calculations). The differential equations of the population balance N_i of the excited Sr II levels have the form:

$$\frac{\mathrm{d}N_i}{\mathrm{d}t} = \sum_{j=0,\, j\neq i}^{20} (A_{ji} + F_{ji} + G_{ji})N_j - \sum_{k=0,\, k\neq i}^{20} (A_{ik} + F_{ik} + G_{ik})N_i - \sum_{i=1}^{20} K^{\mathrm{i}}_{\mathrm{Sr}^{+*}} N_i n_{\mathrm{e}} + \delta_i + W_{\mathrm{p}i}, \quad i = 1 - 20, \qquad (1)$$

where A_{ik} are the probabilities of optical transitions; F_{ik} are the probabilities of the electronic excitation or deexcitation; G_{ik} are the probabilities of the atomic excitation or deexcitation; $K^{\mathrm{i}}_{\mathrm{Sr}^{+*}}$ are the ionisation rate constants of excited states of strontium ions; δ_i are terms taking into account the saturation at laser transitions; and $W_{\mathrm{p}i}$ are partial rates of level pumping.

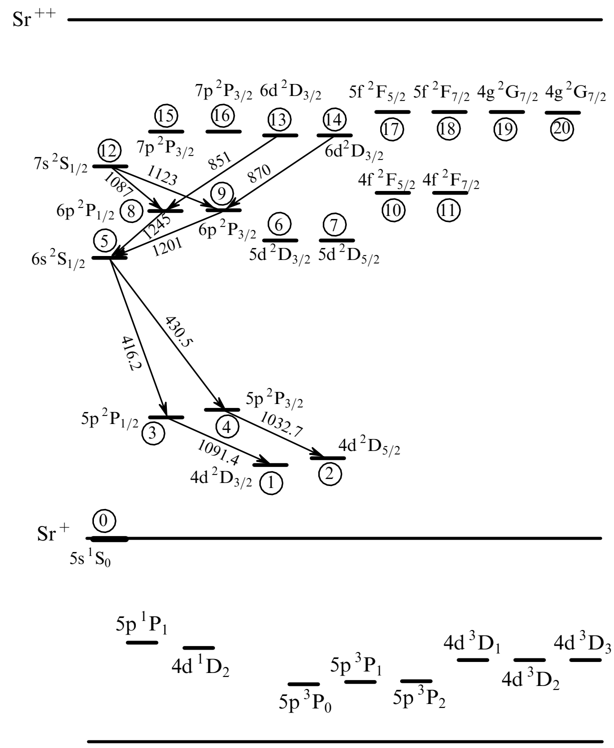

Figure 2. Energy level diagram of strontium atoms and ions (the arrows show the Sr II lasing transitions; the transition wavelengths are given in nanometres; the numbers of the SR II levels used in the mathematic model are shown in circles).

We used parameters close to the experimental conditions: the active element length of 50 cm, its internal diameter of 1.5 cm, the helium pressure of 100 Torr, the initial concentration of strontium atoms of 8.5×10^{14} cm^{-3}, the pulse repetition rate of 15 kHz, the storage capacitance of 100 pF (the discharge scheme was simulated without a peaking capacitor).

Figures 3–6 present the simulation results obtained for single-pulse excitation for the initial voltage across the storage capacitor $U = 8.5$ kV (Figs 3–6a) and for dou-

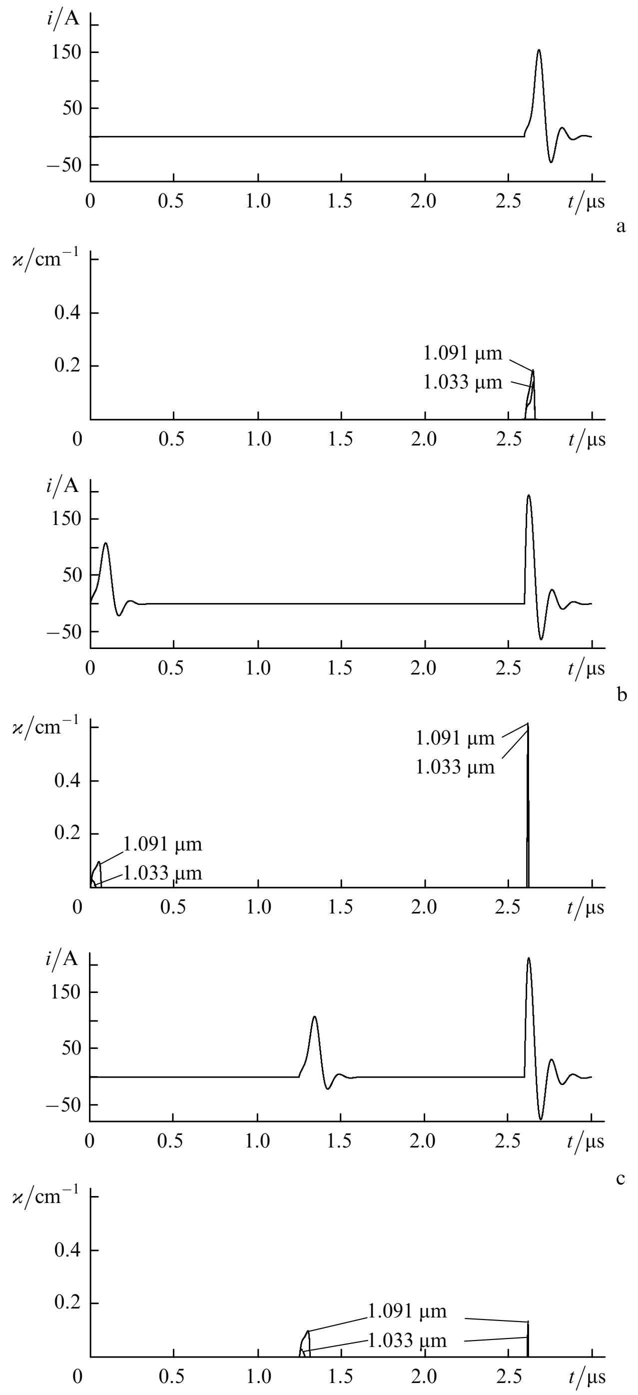

Figure 3. Current pulses i and gains $\varkappa$ at self-contained IR transitions in Sr II ($\lambda = 1.033$ and 1.091 μm) calculated upon single-pulse excitation (a) and two-pulse excitation with delays of 2.6 (b) and 1.35 μs (c) between the additional and excitation pulses.

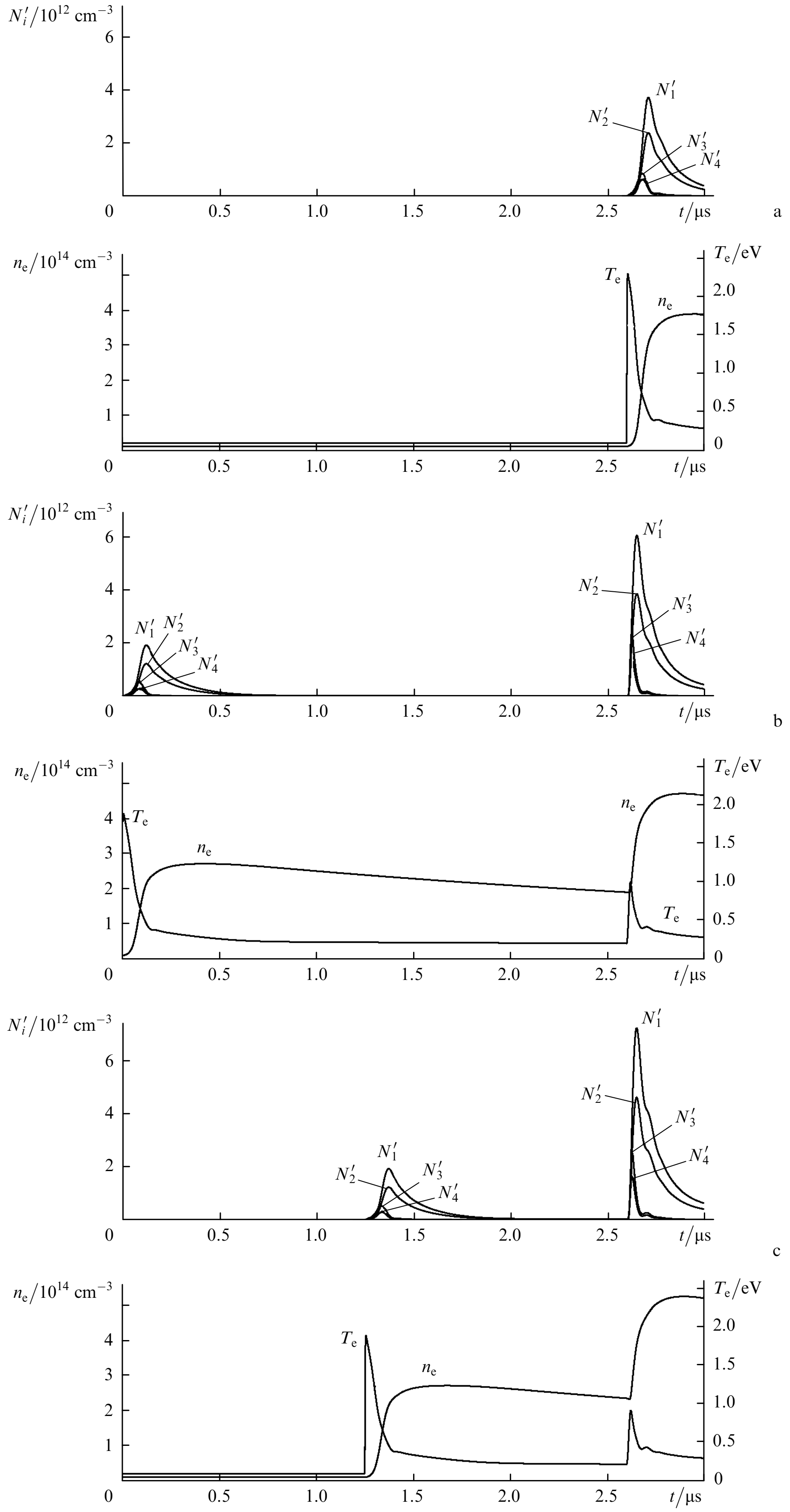

Figure 4. Reduced populations $N_i' = N_i/g_i$ of the working Sr II levels ($\lambda = 1.033$ μm, the $4 \rightarrow 2$ transition and $\lambda = 1.091$ μm, the $3 \rightarrow 1$ transition), the electron concentration n_e and temperature T_e calculated upon single-pulse excitation (a) and two-pulse excitation with delays of 2.6 (b) and 1.35 μs (c) between the additional and excitation pulses.

ble-pulse excitation for $U = 7.2$ kV [for interpulse intervals of 2.6 μs (Figs 3–6b) and 1.35 μs (Figs 3–6c)]. We calculated the discharge current i, the unsaturated gain $\varkappa$ at the IR transitions in Sr II, reduced populations $N_i' = N_i/g_i$ (g_i is the statistical weight of the ith level) of the working 1–4 levels (see the level diagram of Sr II in Fig. 2) and the plasma parameters: the electron concentration n_e and temperature T_e, and concentrations of strontium atoms (N_{Sr}) and ions (N_{Sr^+}). The results of calculations (Fig. 3) agree as a whole with the experimental data (see Fig. 1).

One can see from Fig. 4 that within the time between the pulses, a rather rapid (for less than 1 μs) relaxation of populations N_1, N_2 of metastable Sr II states occurs due to the electronic deexcitation. Note that the high electronic deexcitation rate of Sr II levels favours the inversion formation during the early afterglow at recombination laser transitions ($\lambda = 430.5$ and 416.2 nm) [11, 12, 29, 30].

In the double-pulse regime, the increase in the amplitude and shortening of the second current pulse compared to the first one was observed both in experiments (Fig. 1) and simulations (Fig. 3). This is caused by the presence of a high residual prepulse electron concentration (Fig. 4) and, hence, by a high prepulse conductivity of plasma.

As for amplification, inversion at the leading edge of the current pulse with a rather high gain takes place at both IR transitions in Sr II (Figs 3–5). In the case of two-pulse excitation, amplification in the second pump pulse is higher than in the first one and than in the single-pulse excitation regime.

This is explained by the fact that at a small interpulse interval, the concentration of strontium ions Sr^+, which did not have time to recombine, remains large by the onset of the second pulse (Fig. 6). Accordingly, the fraction of the energy spent to produce Sr^+ ions from the ground state of Sr atoms decreases (Fig. 6) and the excitation efficiency of resonance Sr II levels from its ground state increases. In this case, despite the fact that the increased prepulse concentration n_e prevents rapid heating of the electronic gas and leads to a decrease in T_e in the second current pulse (Fig. 4), the populations of resonance levels and inversion increase (Figs 4 and 5). Thus, the increase in the pump efficiency of resonance Sr II levels in the second pulse results in the increase in the amplification and, as a result, in the growth in the pulse energy characteristics, efficiency and average output power at the IR transitions in Sr II.

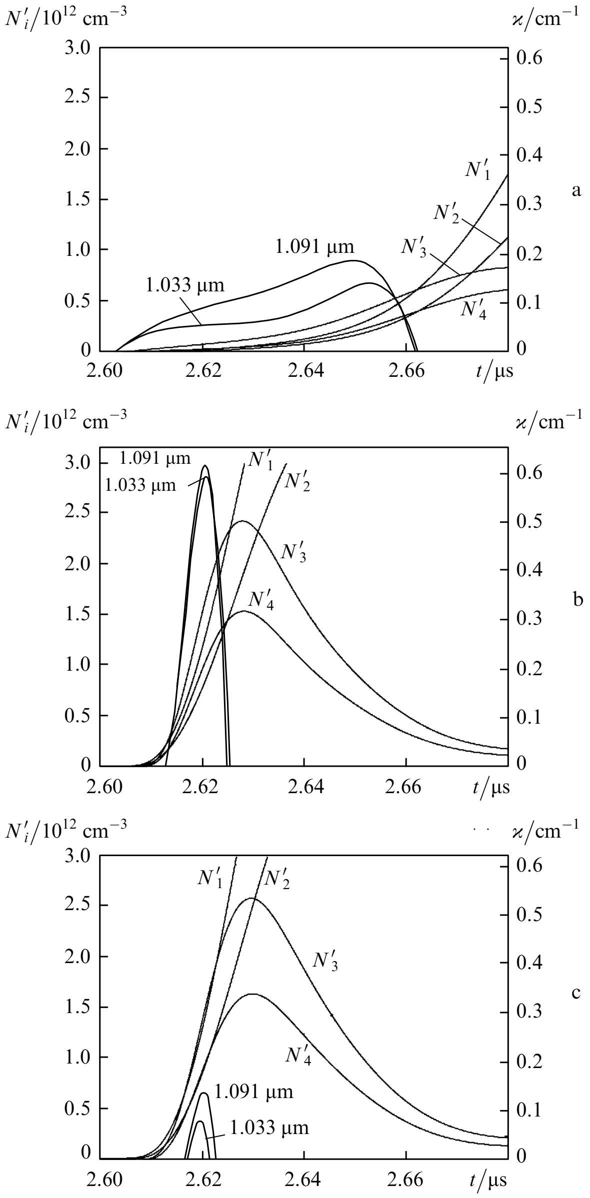

Figure 5. Reduced populations N_i' of the working Sr II levels ($\lambda = 1.033$ μm, the $4 \rightarrow 2$ transition and $\lambda = 1.091$ μm, the $3 \rightarrow 1$ transition) and gains $\varkappa$ at self-contained IR transitions in Sr II ($\lambda = 1.033$ and 1.091 μm) in the excitation pulse calculated upon single-pulse excitation(a) and two-pulse excitation with delays of 2.6 (b) and 1.35 μs (c) between the additional and excitation pulses.

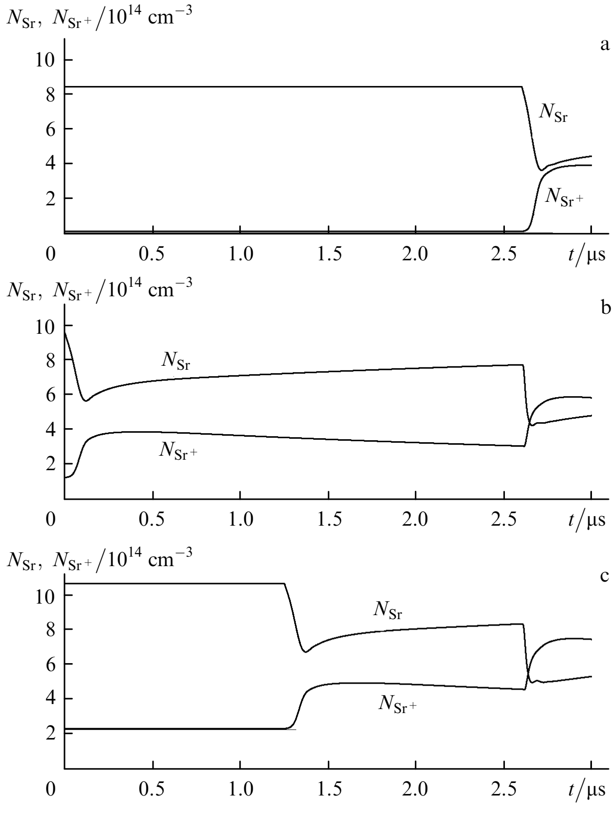

Figure 6. Concentrations of strontium atoms and ions calculated upon single-pulse excitation (a) and two-pulse excitation with delays of 2.6 (b) and 1.35 μs (c) between the additional and excitation pulses.

Note, however, that when the delay between the additional and excitation pulses is decreased (in the delay range from ~ 1 to 3 μs), the laser pulses (Fig. 1) and amplification pulses (Figs 3 and 5) in the excitation pulse shorten and decrease in the amplitude. The decrease in the inversion in the excitation pulse (Figs 4 and 5) is caused by a decrease in T_e caused by the increase in the prepulse concentration of electrons (Fig. 4). It is obvious that when the interpulse interval is further decreased (less than 1 μs), T_e will decrease and approach the value below which the metastable Sr II states will be excited more effectively than the resonance states and inversion does not appear (for example, according to [16, 23], inversion in CVLs disappears at $T_e < 1.7 - 2$ eV, and according to [14] the minimal interpulse interval is ~ 15 μs).

A significant difference of self-contained ion laser is a step excitation character of resonance levels of strontium ions, because of which in the double-pulse regime the increase in the energy output characteristics in the second pulse is possible due to the presence of residual prepulse concentration of Sr^+ strontium ions. In this case, rather low temperature T_e (~ 1 eV) in the second pulse (Fig. 4c), for which inversion still exists (Figs 4 and 5c), is achieved at a rather high prepulse concentration $n_e \sim 2 \times 10^{14}$ cm^{-3} (Fig. 4c), which allows realisation of small interpulse intervals (~ 1 μs). For small delays between pulses (~ 1 μs), the effect of the increasing prepulse population of metastable Sr II states restricting the inversion begins to appear (Figs 4 and 5c). The obtained results indicate the principal possibility of lasing at self-contained IR transitions in Sr II with high pulse repetition rates ($\sim$ 1MHz).

Figure 7 presents the simulation results of two-pulse excitation by varying the interpulse interval in a broad range. One can see that the maximum amplification in the second pulse is achieved for delays $\sim 5 - 10$ μs and exceeds by several times the amplification in the single-pulse excitation regime. When the delays are further increased, the positive effect of rather high residual prepulse concentration of strontium ions decreases and for the delays more than 30 – 50 μs becomes insignificant. These results allow one to predict the optimal pulse repetition rate in trains ($\sim 100 - 200$ kHz).

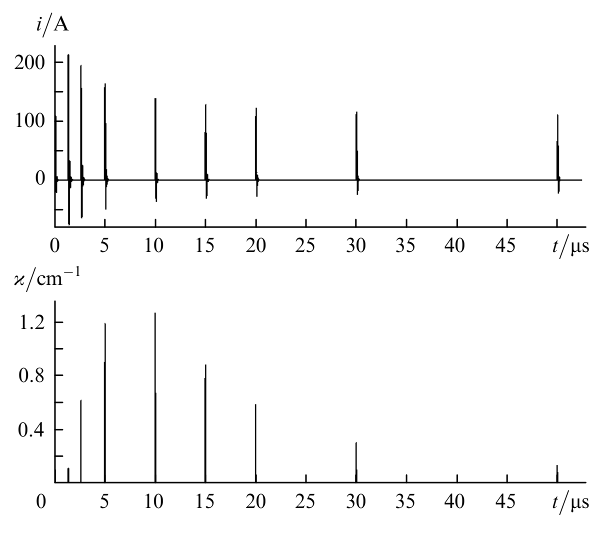

Figure 7. Current pulses i and gains $\varkappa$ at self-contained IR transitions in Sr II calculated upon two-pulse excitation with different delays between the additional and excitation pulses.

Thus, the experimental studies of the self-contained strontium laser and the results of the numerical simulation of the kinetics of processes in its active medium have shown that the laser pulse repetition rate can achieve ~ 1 MHz. It has been found that the laser pulse energy in the second pulse as well as the average power and efficiency increase upon two-pulse excitation in a certain range of time delays between the pulses, caused by the significant prepulse concentration of strontium ions which have no time to recombine. The outlooks for the application of pulse trains to excite self-contained IR transitions of strontium ions have been shown.

References

1. Soldatov A.N., Filonov A.G., Shumeiko A.S., Kirilov A.E., Ivanov B., Haglund R., Mendenhall M., Gabella B., Kostadinov I. *Proc. SPIE Int. Soc. Opt. Eng.*, **5483**, 252 (2004).
2. Gorbunova T.M., Soldatov A.N., Filonov A.G. *Opt. Atmos. Okean.*, **17**, 262 (2004).
3. Soldatov A.N., Filonov A.G., Vasil'eva A.V. *Opt. Atmos. Okean.*, **19**, 224 (2006).
4. Soldatov A.N., Filonov A.G., Polunin Yu.P., Sidorov I.V. *Proc. 8th Sino-Russian Symp. on Laser Physics and Laser Technlogies* (Tomsk, Russia, 2006) p. 26.
5. Soldatov A.N., Polunin Yu.P., Shumeiko A.S., Sidorov I.V. *Proc. 7th Int. Symp. Laser Physics and Laser Technologies* (Tomsk, Russia, 2004) pp 202 – 207.
6. Soldatov A.N., Filonov A.G., Shumeiko A.S., Kuznetsova A.V., Sidorov I.V., Chausova L.N., Polunin Yu.P., Ivanov B., Haglund R., Kostadinov I. *Proc. 7th Int. Symp. Laser Physics and Laser Technologies* (Tomsk, Russia, 2004) pp 32 – 40.
7. Soldatov A.N., Filonov A.G., Vasil'eva A.V. *Tezisy dokl. simp. 'Lazery na parakh metallov'* (Abstracts of Symposium on 'Metal-Vapour Lasers') (Rostov-on-Don, 2006) p. 24.
8. Petrash G.G. *Usp. Fiz. Nauk.*, **105**, 645 (1971).
9. Soldatov A.N., Solomonov V.I. *Gazorazryadnye lazery na samoogranichennykh perekhodakh v parakh metallov* (Gas-Discharge Self-Contained Vapour-Metal Lasers) (Novosibirsk: Nauka, 1985).
10. Batenin V.M., Buchanov V.V., Kazaryan M.A., Klimovskii I.I., Molodykh E.I. *Lazery na samoogranichennykh perekhodakh atomov metallov* (Self-Contained Atomic Metal Lasers) (Moscow: Nauchnaya kniga, 1998).
11. Little C.E. *Metal Vapour Lasers: Physics, Engineering, Applications* (Chichester, New York: John Willey & Sons, 1999).
12. *Entsiklopediya nizkotemperaturnoi plazmy, Gazovye i plazmennye lazery* (Encyclopaedia of Low-Temperature Plasma, Gas and Plasma Lasers) (Moscow: Fizmatlit, 2005) Vol. XI-4.
13. Isaev A.A., Kazakov V.V., Lesnoi M.A., Markova S.V., Petrash G.G. *Kvantovaya Elektron.*, **13**, 2302 (1986) [*Sov. J. Quantum Electron.*, **16**, 1517 (1986)].
14. Isaev A.A., Mikhkel'soo V.T., Petrash G.G., Peet V.E., Ponomarev I.V., Treshchalov A.B. *Kvantovaya Elektron.*, **15**, 2510 (1988) [*Sov. J. Quantum Electron.*, **18**, 1577 (1988)].
15. Petrash G.G. *Proc. SPIE Int. Soc. Opt. Eng.*, **3403**, 110 (1998).
16. Petrash G.G. Preprint FIAN No. 28 (Moscow, 1999).
17. Petrash G.G. *Laser Phys.*, **10**, 994 (2000).
18. Bokhan P.A., Gerasimov V.A., Solomonov V.I., Shcheglov V.B. *Kvantovaya Elektron.*, **5**, 2162 (1978) [*Sov. J. Quantum Electron.*, **8**, 1220 (1978)].
19. Bokhan P.A., Silant'ev V.I., Solomonov V.I. *Kvantovaya Elektron.*, **7**, 1264 (1980) [*Sov. J. Quantum Electron.*, **10**, 724 (1980)].
20. Bokhan P.A. *Kvantovaya Elektron.*, **12**, 945 (1985) [*Sov. J. Quantum Electron.*, **15**, 622 (1985)].
21. Bokhan P.A. *Kvantovaya Elektron.*, **13**, 1837 (1986) [*Sov. J. Quantum Electron.*, **13**, 1207 (1986)].
22. Bokhan P.A., Zakrevskii D.E. *Zh. Tekh. Fiz.*, **67**, 54 (1997).

23. Yakovlenko S.I. *Kvantovaya Elektron.*, **30**, 501 (2000) [*Quantum Electron.*, **30**, 501 (2000)].
24. Boichenko A.M., Evtushenko G.S., Yakovlenko S.I., Zhdaniev O.V. *Laser Phys.*, **11**, 580 (2001).
25. Bokhan P.A., Zakrevskii D.E. *Kvantovaya Elektron.*, **32**, 602 (2002) [*Quantum Electron.*, **32**, 602 (2002)].
26. Yudin N.A. *Opt. Atmos. Okean.*, **19**, 145 (2006).
27. Soldatov A.N. *Opt. Atmos. Okean.*, **6**, 650 (1993).
28. Latush E.L., Chebotarev G.D., Fesenko A.A. *Tezisy dokl. simp. 'Lazery na parakh metallov'* (Abstracts of Symposium 'Metal-Vapour Lasers') (Rostov-on-Don, 2006) pp 33 – 35.
29. Ivanov I.G., Latush E.L., Sem M.F. *Ionnye lazery na parakh metallov* (Metal-Vapour Ion Lasers) (Moscow: Energoatomizdat, 1990).
30. Ivanov I.G., Latush E.L., Sem M.F. *Metal Vapour Ion Lasers: Kinetic Processes and Gas Discharges* (Chichester, New York: John Willey & Sons, 1996).
31. Chebotarev G.D., Prutsakov O.O., Latush E.L. *Proc. SPIE Int. Soc. Opt. Eng.*, **5483**, 83 (2004).